

Response to Editor Dr. Bettina Schaepli

Comments to the Author:

Dear Authors

thanks for the additional detailed revisions. The paper is now ready for publication.

Response:

Thanks for your further comments. We have addressed all and the changes are explained below. We have also carefully read through the paper and made some minor changes in terms of wording.

Non-public comments to the Author:

I have some final technical comments:

Abstract: I am not sure it is possible to have the link to the code in the abstract, ask the editorial team for advice.

Response:

We have emailed the editorial team and asked for their advice. Unfortunately, we have not heard from them yet. But we have checked the guide for authors, and it seems there are no limits on the use of link in the abstract. Our purpose to have the link to the code in the abstract is to give readers a fast way to access the codes if they are interested in this method without reading the whole paper. In order not to miss the deadline for returning the revised copy and also the reasons we explain here, we decide to keep the link at this stage.

The start of the conclusion section is not entirely clear; the sentence “Partial wavelet coherency (PWC) is developed in this study” reads like if this was the first time that this is proposed.

Response:

We changed it to “[Partial wavelet coherency \(PWC\) is improved ...](#)”.

Furthermore, the conclusion suggests that the previously suggested PWC method was wrong whereas only the implementation was wrong.

Current text: In the case of one excluding variable, this new method produces more accurate coherence than the previous PWC method calculation that considered only real coherence rather than complex coherence between every two variables.

Suggestion: In the case of one excluding variable, the PWC implementation provided here (in the paper and the published code) produces more accurate coherence than the previously published PWC implementation that considered wrongly real coherence rather than complex coherence between every two variables

Response:

We changed it as you suggested. Similar changes were also made for the sentence in the abstract. Thanks.

Comments on the math notation:

- There are several instances left where there is dot before the capital Z in the subscript

Response:

The dot is the notation for excluding variables, so we explained it as “[where symbol · is the notation for excluding variables,](#)” to avoid confusion.

- Z1 has the 1 not in the subscript, I hope that the typesetting can correct this

Response:

We've put number 1 into the subscript position for all in the main paper and Supplement. Thanks.

- HESS does not accept /like multi-letter variable names; y_{2wn} and similar are not well chosen, I suggest to use $y_{2,w}$, or $2,m$, $2,s$ or $2,h0$

Response:

We have done as you suggest. For example, they are read as something like $y_{2,h0}$, $y_{2,w}$, $y_{2,w,h0}$, and y_{24} . Changes are made for both main paper and the Supplement. Thanks.

1 Technical Note: Improved partial wavelet coherency for understanding scale-
2 specific and localized bivariate relationships in geosciences

3 Wei Hu¹ and Bing Si²

4 *¹The New Zealand Institute for Plant and Food Research Limited, Private Bag 4704, Christchurch 8140.*

5 *New Zealand*

6 *²University of Saskatchewan, Department of Soil Science, Saskatoon, SK S7N 5A8, Canada*

7 Correspondence to: Wei Hu (wei.hu@plantandfood.co.nz)

8 **Abstract**

9 Bivariate wavelet coherency is a measure of correlation between two variables in the
10 location-scale (spatial data) or time-frequency (time series) domain. It is particularly suited
11 to geoscience where relationships between multiple variables differ with locations (times)
12 and/or scales (frequencies) because of various processes involved. However, it is well-
13 known that bivariate relationships can be misleading when both variables are dependent on
14 other variables. Partial wavelet coherency (PWC) has been proposed to detect scale-specific
15 and localized bivariate relationships by excluding the effects of other variables, but is
16 limited to one excluding variable and provides no phase information. We aim to develop a
17 new PWC method that can deal with multiple excluding variables and provide phase
18 information. Both stationary and non-stationary artificial datasets with the response
19 variable being the sum of five cosine waves at 256 locations are used to test the method.

20 The new method was also applied to a free water evaporation dataset. Our results verified
21 the advantages of the new method in capturing phase information and dealing with multiple
22 excluding variables. Where there is one excluding variable, the new ~~method~~ PWC
23 implementation produces higher and more accurate PWC values than the previously
24 published PWC ~~calculation~~ implementation that mistakenly ~~used~~ considered bivariate real
25 coherence rather than bivariate complex coherence ~~in the calculation~~. We suggest the PWC
26 method is used to untangle scale-specific and localized bivariate relationships after
27 removing the effects of other variables in geosciences. The PWC ~~calculations~~
28 implementations were coded with Matlab and are freely accessible
29 (<https://figshare.com/s/bc97956f43fe5734c784>).

30

31 **1. Introduction**

32 Geoscience data, such as the spatial distribution of soil moisture in undulating terrains
33 and time series of climatic variables, usually consist of a variety of transient processes with
34 different scales or frequencies that may be localized in space or time (Torrence and Compo,
35 1998; Si, 2008; Graf et al., 2014). For example, time series of air temperature usually
36 fluctuates periodically at different scales (e.g., daily and yearly), but abrupt changes in air
37 temperature (e.g., extremely high or low) may occur at certain time points as a result of
38 extreme weather and climate events (e.g., heat and rain). Wavelet methods are widely used
39 to detect localized features of geoscience data.

40 Wavelet analyses are based on the wavelet transform using mother wavelet function,
41 which expands spatial data (or time series) ~~data~~ into location-scale (or time-frequency)
42 space for identification of localized intermittent scales (or frequencies). For convenience,
43 we will mainly refer to location and scale irrespective of spatial or time series data unless
44 otherwise mentioned. Bivariate wavelet coherency (BWC) is widely accepted as a tool for
45 detecting scale-specific and localized bivariate relationships in a range of areas in
46 geoscience (Lakshmi et al., 2004; Si and Zeleke, 2005; Das and Mohanty, 2008; Polansky
47 et al., 2010; Biswas and Si, 2011). The BWC partitions correlation between two variables
48 into different locations and scales, which are different from the overall relationships at the
49 sampling scale as shown by the traditional correlation coefficient. For example, BWC
50 analysis indicated that soil water content of a hummocky landscape in the Canadian Prairies
51 was negatively correlated to soil organic carbon content at a slope scale (50 m), but they
52 were positively correlated at a watershed scale (120 m) in summer because of the different
53 processes involved at different scales (Hu et al., 2017b). Because the positive correlation
54 may cancel out with the negative one at different scales and/or locations, the traditional
55 correlation coefficient between soil water content and soil organic carbon content does not
56 differ significantly from zero, which can be misleading.

57 Recently, Hu and Si (2016) have extended BWC to multiple wavelet coherence (MWC)
58 that can be used to untangle multivariate (≥ 3 variables) relationships in multiple location-
59 scale domains. This method has been successfully used in hydrology (Hu et al., 2017b;
60 Nalley et al., 2019; Su et al., 2019; Gu et al., 2020; Mares et al., 2020) and other areas such
61 as soil science (Centeno et al., 2020), environmental science (Zhao et al., 2018),

62 meteorology (Song et al., 2020), and economics (Sen et al., 2019). The MWC application
63 has shown that an increased number of predictor variables does not necessarily explain
64 more variations in the response variable, partly because predictor variables are usually
65 cross-correlated (Hu and Si, 2016). For the same reason, bivariate relationships can be
66 misleading if the predictor variable is correlated with other variables that control the
67 response variable. Partial correlation analysis is one such method to avoid the misleading
68 relationships resulting from the interdependence between predictor and other variables
69 (Kenney and Keeping, 1939). For example, soil water content of the root zone was found
70 to be positively related to grass yield throughout the year in a small watershed on the
71 Chinese Loess Plateau (Hu et al., 2017a). This was because higher grass yield usually
72 coincided with finer soils that usually have higher water holding capacity. After removing
73 the effects of other factors including sand content, partial correlation analysis indicated that
74 soil water content was negatively affected by grass yield during growing seasons and not
75 affected by grass yield during non-growing seasons as expected. The study of Hu et al.
76 (2017a) clearly demonstrated that partial correlation analysis can be an effective method to
77 avoid misleading relationships between response (e.g., soil water content) and predictor
78 variables (e.g., grass yield) when the latter was interdependent with other variables (e.g.,
79 sand content). However, the extension of partial correlation to the multiple location-scale
80 domain is limited. In order to better understand the bivariate relationships at various scales
81 and locations, BWC needs to be extended to partial wavelet coherency (PWC) by
82 eliminating the effects of other variables.

83 BWC was extended to PWC by Mihanović et al. (2009). Their method has been widely

84 used in the areas of marine science (Ng and Chan, 2012a, b), meteorology (Tan et al., 2016;
85 Rathinasamy et al., 2017), and economics (Aloui et al., 2018; Altarturi et al., 2018a; Wu et
86 al., 2020), as well as in the study of greenhouse gas emissions (Jia et al., 2018; Li et al.,
87 2018; Mutascu and Sokic, 2020), among others. For example, PWC analysis indicated that
88 the Southern Oscillation Index and Pacific Decadal Oscillation did not affect precipitation
89 across India, while this was misinterpreted by the BWC analysis because of their
90 interdependence on Niño 3.4, which affects precipitation (Rathinasamy et al., 2017).
91 Unfortunately, the PWC ~~calculation~~implementation in many previous studies (Ng and
92 Chan, 2012b; Rathinasamy et al., 2017; Aloui et al., 2018; Altarturi et al., 2018b; Jia et al.,
93 2018; Li et al., 2018; Mutascu and Sokic, 2020; Wu et al., 2020) was based on an incorrect
94 Matlab code developed by Ng and Chan (2012a) who might have misinterpreted the
95 equation of Mihanović et al. (2009) and mistakenly used bivariate real coherence rather
96 than bivariate complex coherence for calculating PWC. Moreover, Mihanović et al. (2009)
97 considered only one excluding variable (i.e., the variable that influences the response
98 variable is excluded) and did not include the phase angle difference between response and
99 predictor variables. The PWC values between response and predictor variables can still be
100 misleading if more than one variable is interdependent with the predictor variable. This is
101 especially true if these variables are correlated with the predictor variable at different
102 locations and/or scales. Without phase information, it is hard to tell if the correlation at a
103 location and scale is positive or negative.

104 As an extension of previous studies (Mihanović et al., 2009; Hu and Si, 2016), this paper
105 aims to develop a PWC method that considers more than one excluding variable and

106 provides phase information. This new method reveals the magnitude and type of bivariate
107 relationships after removing the effects from all potentially interdependent variables. We
108 expect that the new method produces more accurate PWC values than the
109 ~~implementation~~ of Ng and Chan (2012a) where there is one excluding variable.
110 The new method is an extension of the multivariate partial coherency in the frequency (scale)
111 domain (Koopmans, 1995). The proposed method is first tested with artificial datasets
112 following Yan and Gao (2007) and Hu and Si (2016) to demonstrate its capability of
113 capturing the known relationships of the artificial data. Then it is applied to a real dataset,
114 i.e., time series of free water evaporation at the Changwu site in China (Hu and Si, 2016).
115 Finally, the advantages and weaknesses of the new method are discussed by comparing it
116 with the previous PWC method (Mihanović et al., 2009) and ~~implementation~~
117 (Ng and Chan, 2012a).

118 **2. Theory**

119 Wavelet analysis is based on the wavelet transform, which includes continuous wavelet
120 transform and discrete wavelet transform. While the discrete wavelet transform is mainly
121 used for data compression and noise reduction, the continuous wavelet transform is widely
122 used for extracting scale-specific and localized features, as in the case of this study
123 (Grinsted et al., 2004). The wavelet transform decomposes the spatial ~~data~~ (or time series)
124 ~~data~~ into a set of location- and scale-specific wavelet coefficients, which are scaled
125 (contracted or expanded) and shifted versions of mother wavelets. Different mother
126 wavelets are available for wavelet transform. Among which, the Morlet wavelet, composed

127 of a complex exponential multiplied by a Gaussian window, provides a good balance
128 between location and scale localization. Therefore, continuous wavelet transform with the
129 Morlet wavelet is suitable to transform spatial data (or time series) data into a location-scale
130 (or time-frequency) domain, which allows us to identify both location-specific amplitude
131 and phase information of wavelet coefficients at different scales (Torrence and Compo,
132 1998). Wavelet coefficients and their complex conjugates are used to calculate auto-wavelet
133 power spectra and cross-wavelet power spectra. BWC is calculated as the ratio of smoothed
134 cross-wavelet power spectra of two variables to the product of their auto-wavelet power
135 spectra (Grinsted et al., 2004). Hu and Si (2016) extended wavelet coherence from two to
136 multiple (≥ 3) variables and developed MWC. Detailed information on the calculations of
137 wavelet coefficients, auto- and cross-wavelet power spectra, BWC, and MWC based on the
138 continuous wavelet transform can be found in previous studies (e.g., Torrence and Compo,
139 1998; Grinsted et al., 2004; Si and Farrell, 2004; Si, 2008; Hu and Si, 2016; Hu et al.,
140 2017b). Here, we will only introduce the theory and calculation that are most relevant to
141 PWC.

142 Similar to BWC and MWC, PWC is calculated from auto- and cross-wavelet power
143 spectra, for the response variable y , predictor variable x , and excluding variables Z
144 ($Z = \{Z_1, Z_2, \dots, Z_q\}$). Koopmans (1995) developed the multivariate complex PWC in the
145 frequency (scale) domain. Here, we extend the Koopmans (1995) method from the
146 frequency (scale) domain to the time-frequency (location-scale) domain. Therefore, the
147 complex PWC between y and x after excluding variables Z at scale s and location
148 τ , $\gamma_{y,x \cdot Z}(s, \tau)$, can be written as

$$149 \quad \gamma_{y,x,z}(s, \tau) = \frac{(1 - R_{y,x,z}^2(s, \tau)) \gamma_{y,x}(s, \tau)}{\sqrt{(1 - R_{y,z}^2(s, \tau))(1 - R_{x,z}^2(s, \tau))}} \quad (1)$$

150 Wherever symbol \cdot is the notation for excluding variables; $-R_{yx,z}^2(s, \tau)$, $R_{y,z}^2(s, \tau)$,
 151 and $R_{x,z}^2(s, \tau)$ can be calculated by following Hu and Si (2016) as

$$152 \quad R_{y,x,z}^2(s, \tau) = \frac{\overleftrightarrow{W}^{y,z}(s, \tau) \overleftrightarrow{W}^{z,z}(s, \tau)^{-1} \overleftrightarrow{W}^{x,z}(s, \tau)}{\overleftrightarrow{W}^{y,x}(s, \tau)} \quad (2)$$

$$153 \quad R_{y,z}^2(s, \tau) = \frac{\overleftrightarrow{W}^{y,z}(s, \tau) \overleftrightarrow{W}^{z,z}(s, \tau)^{-1} \overleftrightarrow{W}^{y,z}(s, \tau)}{\overleftrightarrow{W}^{y,y}(s, \tau)} \quad (3)$$

$$154 \quad R_{x,z}^2(s, \tau) = \frac{\overleftrightarrow{W}^{x,z}(s, \tau) \overleftrightarrow{W}^{z,z}(s, \tau)^{-1} \overleftrightarrow{W}^{x,z}(s, \tau)}{\overleftrightarrow{W}^{x,x}(s, \tau)} \quad (4)$$

155 Eq. (1) can be also derived analogously from the complex partial spectrum for the frequency
 156 domain according to the definition of complex coherence between two variables in the time-
 157 frequency domain (see the Supplement (Sect. S1) for the derivation process). Note that
 158 $R_{y,x,z}^2(s, \tau)$ is a matrix with complex values, while $R_{y,z}^2(s, \tau)$ and $R_{x,z}^2(s, \tau)$ are matrices
 159 with real numbers. $\gamma_{y,x}(s, \tau)$ is the complex wavelet coherence between y and x , which
 160 can be written as

$$161 \quad \gamma_{y,x}(s, \tau) = \frac{\overleftrightarrow{W}^{y,x}(s, \tau)}{\left(\overleftrightarrow{W}^{y,y}(s, \tau) \overleftrightarrow{W}^{x,x}(s, \tau)\right)^{1/2}} \quad (5)$$

162 where $\overleftrightarrow{(\cdot)}$ is the smoothing operator, $\overline{(\cdot)}$ is the complex conjugate operator, $(\cdot)^{-1}$
 163 indicates the inverse of the matrix, and

164
$$\leftrightarrow_W^{y,Z}(s, \tau) = \left[\leftrightarrow_W^{y,Z_1}(s, \tau) \leftrightarrow_W^{y,Z_2}(s, \tau) \cdots \leftrightarrow_W^{y,Z_q}(s, \tau) \right] \quad (6)$$

165
$$\leftrightarrow_W^{x,Z}(s, \tau) = \left[\leftrightarrow_W^{x,Z_1}(s, \tau) \leftrightarrow_W^{x,Z_2}(s, \tau) \cdots \leftrightarrow_W^{x,Z_q}(s, \tau) \right] \quad (7)$$

166
$$\leftrightarrow_W^{Z,Z}(s, \tau) = \begin{bmatrix} \leftrightarrow_W^{Z_1,Z_1}(s, \tau) & \cdots & \leftrightarrow_W^{Z_1,Z_q}(s, \tau) \\ \vdots & \ddots & \vdots \\ \leftrightarrow_W^{Z_q,Z_1}(s, \tau) & \cdots & \leftrightarrow_W^{Z_q,Z_q}(s, \tau) \end{bmatrix} \quad (8)$$

167 where $\leftrightarrow_W^{A,B}(s, \tau)$ is the smoothed auto-wavelet power spectra (when $A=B$) or cross-
 168 wavelet power spectra (when $A \neq B$) at scale s and location $-\tau$, respectively.

169 The squared PWC (hereinafter referred to as PWC) at scale s and location $-\tau$, $\rho_{y,x,Z}^2$,
 170 can be written as

171
$$\rho_{y,x,Z}^2 = \frac{|1 - R_{y,x,Z}^2(s, \tau)|^2 R_{y,x}^2(s, \tau)}{(1 - R_{y,Z}^2(s, \tau))(1 - R_{x,Z}^2(s, \tau))} \quad (9)$$

172 where $R_{y,x}^2(s, \tau)$ is squared BWC between y and x , which can be expressed as

173
$$R_{y,x}^2(s, \tau) = \frac{\overline{\leftrightarrow_W^{y,x}(s, \tau)} \leftrightarrow_W^{y,x}(s, \tau)}{\overline{\leftrightarrow_W^{y,y}(s, \tau)} \overline{\leftrightarrow_W^{x,x}(s, \tau)}} \quad (10)$$

174 The phase angle (i.e., angle between two complex numbers) between y and x after
 175 excluding effect of Z is

176
$$\vartheta_{y,x,Z}(s, \tau) = \varphi_{y,x,Z}(s, \tau) + \vartheta_{y,x}(s, \tau) \quad (11)$$

177 where

178
$$\varphi_{y,x,Z}(s, \tau) = \arg(1 - R_{y,x,Z}^2(s, \tau)) \quad (12)$$

179 and $\vartheta_{y,x}(s, \tau)$ is the wavelet phase between y and x , which can be expressed as

180 $\vartheta_{y,x}(s, \tau) = \tan^{-1} \left(\text{Im}(W^{y,x}(s, \tau)) / \text{Re}(W^{y,x}(s, \tau)) \right) \quad (13)$

181 where \arg denotes the argument of the complex number, $W^{y,x}(s, \tau)$ is the cross-wavelet
 182 power spectrum between y and x at scale s and location τ ; Im and Re denote the
 183 imaginary and real part of $W^{y,x}(s, \tau)$, respectively.

184 When only one variable (e.g., $Z_{1\pm}$) is excluded, Eq.(9) can be written as (see the
 185 Supplement (Sect. S2) for the derivation process)

186
$$\rho_{y,x:Z_{1\pm}}^2 = \frac{|\gamma_{y,x}(s,\tau) - \gamma_{y,Z_{1\pm}}(s,\tau)\overline{\gamma_{x,Z_{1\pm}}(s,\tau)}|^2}{(1-R_{y,Z_{1\pm}}^2(s,\tau))(1-R_{x,Z_{1\pm}}^2(s,\tau))} \quad (14)$$

187 The widely used Monte Carlo method (Torrence and Compo, 1998; Grinsted et al., 2004;
 188 Si and Farrell, 2004) is used to calculate PWC at the 95% confidence level. In brief, the
 189 PWC calculation is repeated for a sufficient number (i.e., minimum number required) of
 190 times using data generated by Monte Carlo simulations based on the first-order
 191 autocorrelation coefficient (r_1). The first-order autoregressive model (AR(1)) is chosen
 192 because most geoscience data can be effectively simulated by it (Wendroth et al., 1992;
 193 Grinsted et al., 2004; Si and Farrell, 2004), although we recognize that time series with
 194 long-range dependence is also common in many areas such as hydrology (Szolgayová et
 195 al., 2014). Different combinations of r_1 values (i.e., 0.0, 0.5, and 0.9) were used to generate
 196 10 to 10 000 AR(1) series with three, four and five variables. Our results indicate that the
 197 noise combination has little impact on the PWC values at the 95% confidence level as also
 198 found by Grinsted et al. (2004) for the BWC case (data not shown). The relative difference
 199 of PWC at the 95% confidence level compared with that calculated from the 10 000 AR(1)

200 series decreases with the increase in number of AR(1) series (Fig. S1 of Sect. S3 in the
 201 Supplement). When the number of AR(1) is above 300, a very low maximum relative
 202 difference (e.g., <2%) is observed. Therefore, a repeating number of 300 seems to be
 203 sufficient for a significance test. However, if calculation time is not a barrier, a higher
 204 repeating number, such as ≥ 1000 , is recommended. The 95th percentile of PWCs of all
 205 simulations at each scale represents PWC at the 95% confidence level. The average PWC,
 206 percent area of significant coherence (PASC) relative to the whole wavelet location–scale
 207 domain (Hu and Si, 2016), and average value of significant PWC (PWC_{sig}) are also
 208 calculated for different location–scale domains.

209 In the case of one excluding variable ($Z = \{Z_1\}$), Mihanović et al. (2009) suggested that
 210 PWC can be calculated by an equation analogous to the traditional partial correlation
 211 squared (Kenney and Keeping, 1939) without giving detailed derivation process. Their
 212 equation is the same as Eq. (14). Unfortunately, Ng and Chan (2012a) might have
 213 misinterpreted the equation of Mihanović et al. (2009) and developed Matlab code for
 214 calculating PWC using the equation expressed as

$$215 \quad \rho_{y,x,Z_1}^2 = \frac{|R_{y,x}(s,\tau) - R_{y,Z_1}(s,\tau) R_{x,Z_1}(s,\tau)|^2}{(1 - R_{y,Z_1}^2(s,\tau))(1 - R_{x,Z_1}^2(s,\tau))} \quad (15)$$

216 where $R_{y,x}(s,\tau)$, $R_{y,Z_1}(s,\tau)$, and $R_{x,Z_1}(s,\tau)$ are the square root of $R_{y,x}^2(s,\tau)$,
 217 $R_{y,Z_1}^2(s,\tau)$, $R_{x,Z_1}^2(s,\tau)$, respectively. $R_{y,Z_1}^2(s,\tau)$ and $R_{x,Z_1}^2(s,\tau)$ can be
 218 calculated from Eq. (10) by replacing y and x with their corresponding variables. Eq.
 219 (15) has been widely used to calculate PWC in the case of one excluding variable (Ng and

220 Chan, 2012b; Rathinasamy et al., 2017; Aloui et al., 2018; Altarturi et al., 2018b; Jia et al.,
 221 2018; Li et al., 2018; Mutascu and Sokic, 2020; Wu et al., 2020). Note that complex
 222 coherence and real coherence are involved in the numerators of Eqs. (14) and (15),
 223 respectively, while the denominators are exactly the same. Further comparison indicates
 224 that Eq. (15) underestimates PWC value relative to Eq. (14) unless $\gamma_{y,x}(s, \tau)$
 225 and $\gamma_{y,z_1 z_4}(s, \tau) \overline{\gamma_{x,z_1 z_4}(s, \tau)}$ in Eq. (14) are collinear (i.e., their arguments are identical)
 226 under which the two equations produce the same PWC values. Differences between Eqs.
 227 (14) and (15) will be discussed further using both artificial data and a real dataset. For
 228 comparison purposes, we refer to Eqs. (14) and (15) as the new calculation-implementation
 229 and the classical calculation-implementation, respectively.

230 **3. Method test using artificial data**

231 **3.1 Artificial data and analysis**

232 PWC is first tested using the cosine-like artificial dataset produced following Yan and
 233 Gao (2007). The cosine-like artificial datasets are suitable for testing the new method
 234 because they mimic many spatial or time series data in geoscience such as climatic variables,
 235 hydrologic fluxes, seismic signals, El Niño-Southern Oscillation, land surface topography,
 236 ocean waves, and soil moisture. The procedures to test PWC are largely based on Hu and
 237 Si (2016), where the same dataset has been used to test the MWC method (refer to Hu and
 238 Si (2016) for a detailed description of the artificial dataset). The response variable (y and z
 239 for the stationary and non-stationary case, respectively) is the sum of five cosine waves (y_1
 240 to y_5 and z_1 to z_5 for the stationary and non-stationary case, respectively) at 256 locations

241 (Hu and Si, 2016). For y_1 to y_5 , they have consistent dimensionless scales of 4, 8, 16, 32,
 242 and 64, respectively, across the series. From z_1 to z_5 , the dimensionless scales gradually
 243 change with location, with the maximum dimensionless scales of 4, 8, 16, 32, and 64,
 244 respectively. The variance of the response variable y and z is 2.5. All other variables are
 245 orthogonal to each other with equal variance of 0.5. The predictor and excluding variables
 246 (Fig. S1 of Sect. S4 in the Supplement) are selected from two of the five cosine waves (i.e.,
 247 y_2 and y_4 or z_2 and z_4) and/or their derivatives. The exact variables and procedures to test
 248 the new PWC method are explained below.

249 First, PWC between response variable y (or z) and predictor variable, i.e., y_2 (or z_2), is
 250 calculated after excluding the effect of one variable. Four types of excluding variable are
 251 involved (Fig. S2 of Sect. S4 in the Supplement): (a) original series of y_4 (or z_4); (b) second
 252 half of the original series of y_2 (or z_2) are replaced by 0 to simulate abrupt changes (i.e.,
 253 transient and localized feature) of the spatial data. They are referred to as $y_{2,h0}h0$ (or $z_{2,h0}z_{2,h0}$);
 254 (c) white noises with zero-mean and standard deviations of 0.3 (weak noise), 1 (moderate
 255 noise), and 4 (high noise) are added to y_2 (or z_2) as suggested by Hu and Si (2016) to
 256 simulate non-perfect cyclic patterns of the excluding variables. They are referred to as
 257 $y_{2,w}w$ (or $z_{2,w}w$), $y_{2,m}m$ (or $z_{2,m}m$), and $y_{2,s}s$ (or $z_{2,s}s$), respectively; and (d) a
 258 combination of type b and type c. They are referred to as $y_{2,w,h0}w$ (or $z_{2,w,h0}z_{2,w,h0}$),
 259 $y_{2,m,h0}m$ (or $z_{2,m,h0}z_{2,m,h0}$), and $y_{2,s,h0}s$ (or $z_{2,s,h0}z_{2,s,h0}$), respectively.

260 Second, PWC between response variable y (or z) and predictor variable, i.e., y_{2+4} (sum
 261 of y_2 and y_4) for the stationary case or z_{2+4} (sum of z_2 and z_4) for the non-stationary case, is

262 calculated with two excluding variables, which is a combination of y_4 (or z_4) and y_2 (or z_2)
263 or its noised series ($y_{2,w}^{###}$ or $z_{2,w}^{###}$, $y_{2,m}^{###}$ or $z_{2,m}^{###}$, and $y_{2,s}^{###}$ or $z_{2,s}^{###}$).

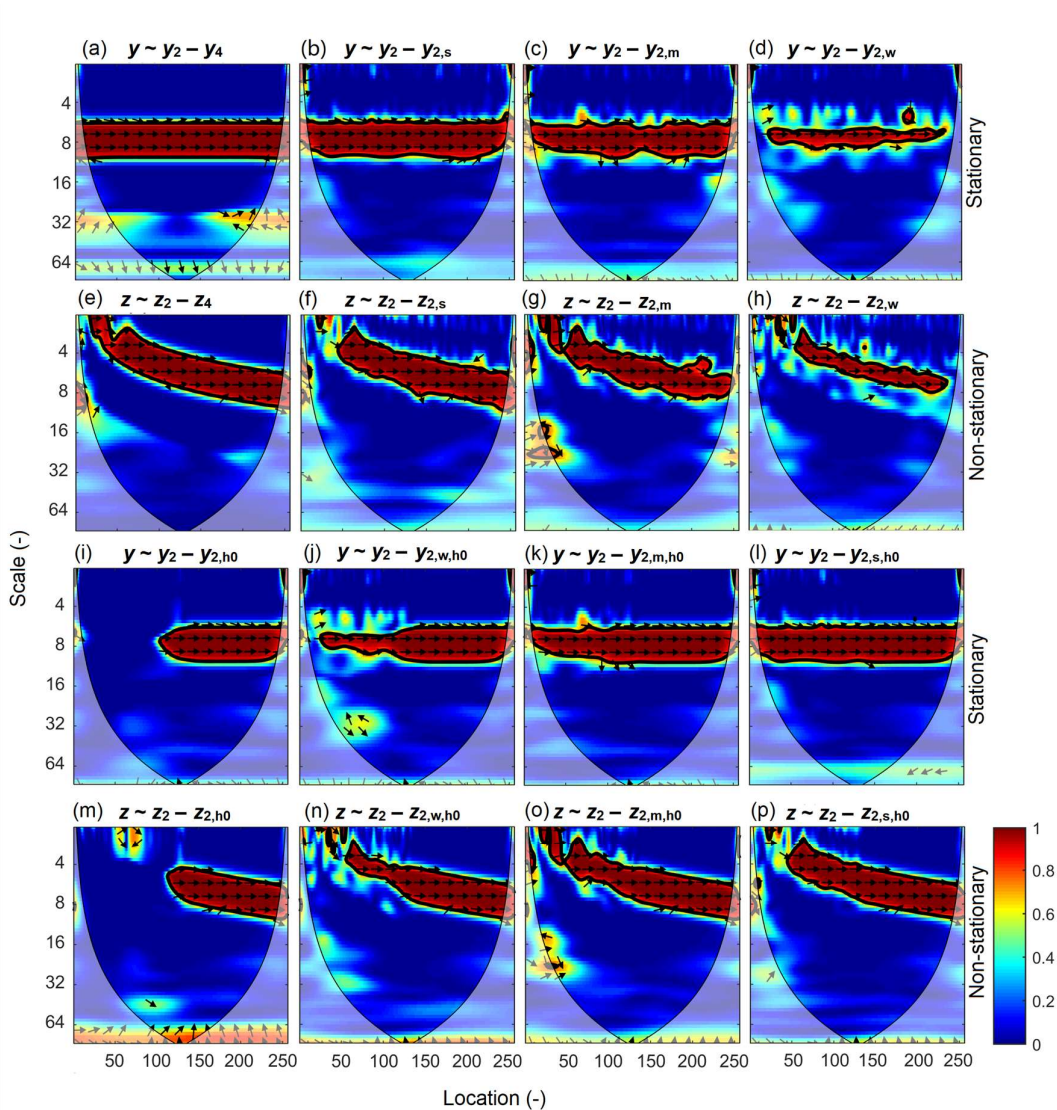
264 The merit of the artificial data is that we know the exact scale-specific and localized
265 bivariate relationships after the effect of excluding variables is removed. Theoretically, we
266 expect (a) PWC is 1 at scales corresponding to relative complement of excluding variable
267 scales in predictor variable scales, and 0 at other scales. For example, PWC between y and
268 $y_{24}^{y_4}$ after excluding the effect of y_4 is expected to be 1 at the scale of 8, which is the relative
269 complement of scale of excluding variable y_4 (32) in scales of predictor variable $y_{24}^{y_4}$ (8
270 and 32), and 0 at other scales; (b) PWC remains 1 at the second half of series where spatial
271 series is replaced by 0, and 0 at the first half of the original series. For example, PWC
272 between y and y_2 after excluding the effect of $y_{2,h_0}^{h_0}$ is expected to be 0 and 1 at the first
273 and second half of series, respectively, at the scale of 8; and (c) PWC increases as more
274 noises are included in the excluding variables. For example, PWC between y and y_2 after
275 excluding the effect of noised series of y_2 is expected to increase with increasing noises in
276 an order of $y_{2,s}^{###} > y_{2,m}^{###} > y_{2,w}^{###}$ at the scale of 8.

277 3.2 PWC with artificial data

278 3.2.1 PWC with one excluding variable using the new method

279 Fig. 1 shows PWC between response variable y (or z) and predictor variable y_2 (or z_2) by
280 excluding one variable. For the stationary case, there is one horizontal band (red color)
281 representing an in-phase high PWC value at scales around 8 for all locations after

282 eliminating the effect of y_4 (Fig. 1a). Note that the PWC values between y and y_2 after
283 excluding the effect of y_4 are not exactly 1 as would be expected at all location-scale
284 domains, because of the effect of smoothing along locations and scales. However, the PWC
285 values at the center of the significance band, which corresponds to the predictor variable y_2
286 at exactly the scale of 8, are very close to 1 (0.996), and the mean PWC_{sig} values are very
287 high (i.e., 0.96). The result is similar to the BWC between y and y_2 (data not shown). This
288 is understandable because y_4 is orthogonal to y_2 , and excluding the effect of y_4 does not
289 affect the relationship between y and y_2 at all.—



290

291 **Figure 1.**

292 Partial wavelet coherency (PWC) between response variable y (or z) and predictor variable
 293 y_2 (or z_2) after excluding the effect of variables y_4 (or z_4), $y_{2,s}$ (or $z_{2,s}$), $y_{2,m}$ (or $z_{2,m}$),
 294 $y_{2,w}$ (or $z_{2,w}$), y_{2,h_0} (or z_{2,h_0}), y_{2,w,h_0} (or z_{2,w,h_0}), y_{2,m,h_0} (or z_{2,m,h_0}),
 295 and y_{2,s,h_0} (or z_{2,s,h_0}) for the stationary (or non-stationary) case using the new
 296 method. Arrows represent the phase angles of the cross-wavelet power spectra between two
 297 variables after eliminating the effect of excluding variables. Arrows pointing to the right
 298 (left) indicate positive (negative) correlations. Thin and thick solid lines show the cones of
 299 influence and the 95% confidence levels, respectively. All variables were generated by

300 following Yan and Gao (2007) and Hu and Si (2016) and are explained in Section 3.1 and
301 shown in Fig. S2 of Sect. S3 in the Supplement.

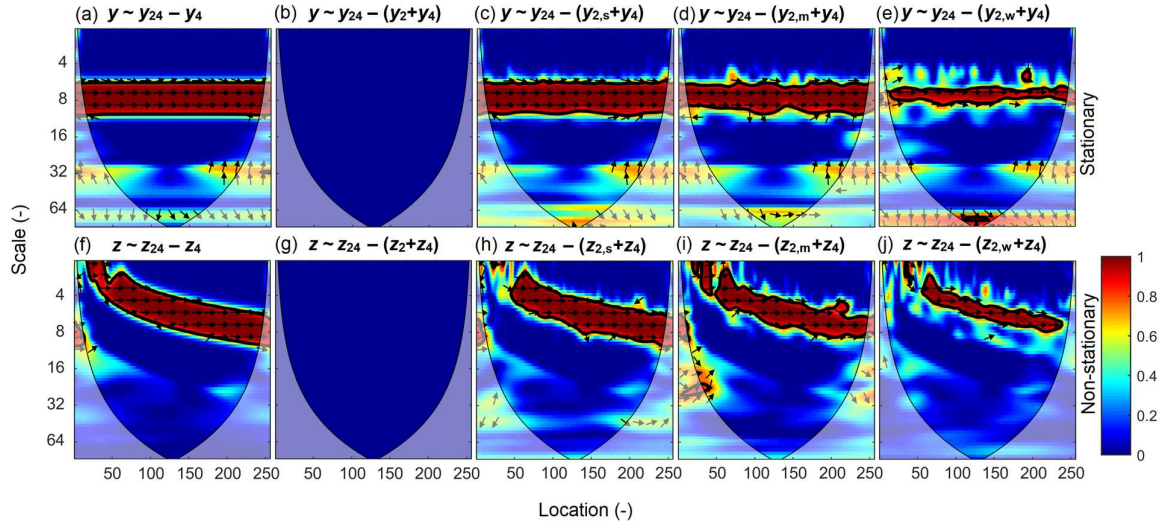
302 Compared with the case of excluding variable of y_4 (Fig. 1a), excluding the effect of
303 $y_{2_s\#}$ (Fig. 1b) results in slightly narrower band of significant PWC and slightly reduced
304 mean PWC_{sig} (0.94 versus 0.96). When less noise is included in the excluding variables (i.e.,
305 $y_{2_m\#\#}$ and $y_{2_w\#\#}$) (Fig. 1c-d), the significant PWC band becomes narrower. The PASC
306 values are 86%, 77%, and 32% for excluding $y_{2_s\#}$, $y_{2_m\#\#}$ and $y_{2_w\#\#}$, respectively, at
307 scales of 6–10. Moreover, the mean PWC_{sig} decreases from 0.94 ($y_{2_s\#}$) to 0.93 ($y_{2_m\#\#}$)
308 and 0.89 ($y_{2_w\#\#}$) when progressively less noise is added (Fig. 1b-d). For the non-stationary
309 case, similar results are obtained (Fig. 1e-h). The only difference is that the scales with
310 significant PWC values change with location, as is found for MWC (Hu and Si, 2016).

311 When the second half of the excluding variable series is replaced by 0, the PWC values
312 in that half are close to 1, while those in the first half of data series are 0 at scales
313 corresponding to the predictor variable (Fig. 1i and 1m). For the stationary case, after
314 excluding the effect of $y_{2_h0\#0}$, the PWC values are close to 1 (0.98) and 0 in the second and
315 first half of the data series, respectively, at the dimensionless scale of 8 (Fig. 1i). Similar
316 results are observed for the non-stationary case (Fig. 1m). This is anticipated because the
317 series of 0s is independent of the predictor variable and hence has no effect on the
318 correlations between response and predictor variables at these locations. If different
319 magnitudes of noises are added to the first half of the excluding variables (y_2 or z_2), the
320 significant PWC band in the first half becomes wider as the magnitude of noises increases,
321 while the significant PWC band in the second half remains almost unchanged (Fig. 1j-l and

322 Fig. 1n-p). In the stationary case, for example, the PASC values at scales of 6–10 are 40%
 323 ($y_{2,w,h0}$), 74% ($y_{2,m,h0}$), and 86% ($y_{2,s,h0}$) in the first half, while those values
 324 vary from 86% to 90% in the second half (Fig. 1j-l). Meanwhile, the mean PWC_{sig} in the
 325 first half at scales of 6–10 increases from 0.91 to 0.94 in both the stationary (Fig. 1j-l) and
 326 non-stationary (Fig. 1n-p) cases as more noises are added to the excluding variable y_2 or z_2 .
 327 This indicates that the new PWC method can also capture the abrupt changes (Fig. 1i and
 328 1m) in the data series, and has the ability to deal with localized relationships.

329 3.2.2 PWC with two excluding variables using the new method

330 When both y_2 and y_4 (or z_2 and z_4) are considered in the predictor variables, there are two
 331 bands of wavelet coherence of 1 between y (or z) and $y_{2,4}$ (or $z_{2,4}$) (Hu and Si, 2016),
 332 which correspond to the scales of two predictor variables. However, after the effect of y_4
 333 (or z_4) is removed, only one band with PWC of around 1 occurs at the scale of the predictor
 334 variable y_2 (or z_2) (Fig. 2a and 2f). After both predictor variables y_2 and y_4 (or z_2 and z_4) are
 335 excluded (Fig. 2b and 2g), PWC between y (or z) and $y_{2,4}$ (or $z_{2,4}$) is 0 at all location-
 336 scale domains as expected. When one of the excluding variables y_2 (or z_2) is added with
 337 noises, the relationship between response variable y (or z) and predictor variable $y_{2,4}$ (or
 338 $z_{2,4}$) becomes significant at scales of the excluding variable y_2 (or z_2) (Fig. 2c and 2h).
 339 Similar to the case of one excluding variable (Fig. 1), less noise in the excluding variable
 340 of y_2 (or z_2) results in a narrower significant PWC band, and reduced mean PWC_{sig} values,
 341 e.g., from 0.96 ($y_{2,s}$) to 0.90 ($y_{2,w}$) in the stationary case (Fig. 2c-e) and from 0.95 ($z_{2,s}$)
 342 to 0.92 ($z_{2,w}$) in the non-stationary case (Fig. 2h-j).



343

344 **Figure 2.**

345 Partial wavelet coherency (PWC) between response variable y (or z) and predictor variable
 346 $y_{24}+y_4$ (or $z_{24}+z_4$) after excluding the effect of variables y_4 (or z_4), y_{2+y_4} (or z_{2+z_4}), $y_{2,sSH}+y_4$ (or
 347 $z_{2,sSH}+z_4$), $y_{2,mSH}+y_4$ (or $z_{2,mSH}+z_4$), and $y_{2,wSH}+y_4$ (or $z_{2,wSH}+z_4$) for the stationary (or non-
 348 stationary) case using the new method. All variables were generated by following Yan and
 349 Gao (2007) and Hu and Si (2016) and are explained in Sect. 3.1 and shown in Fig. S2 of
 350 Sect. S3 in the Supplement.

351 4. Method application with real dataset

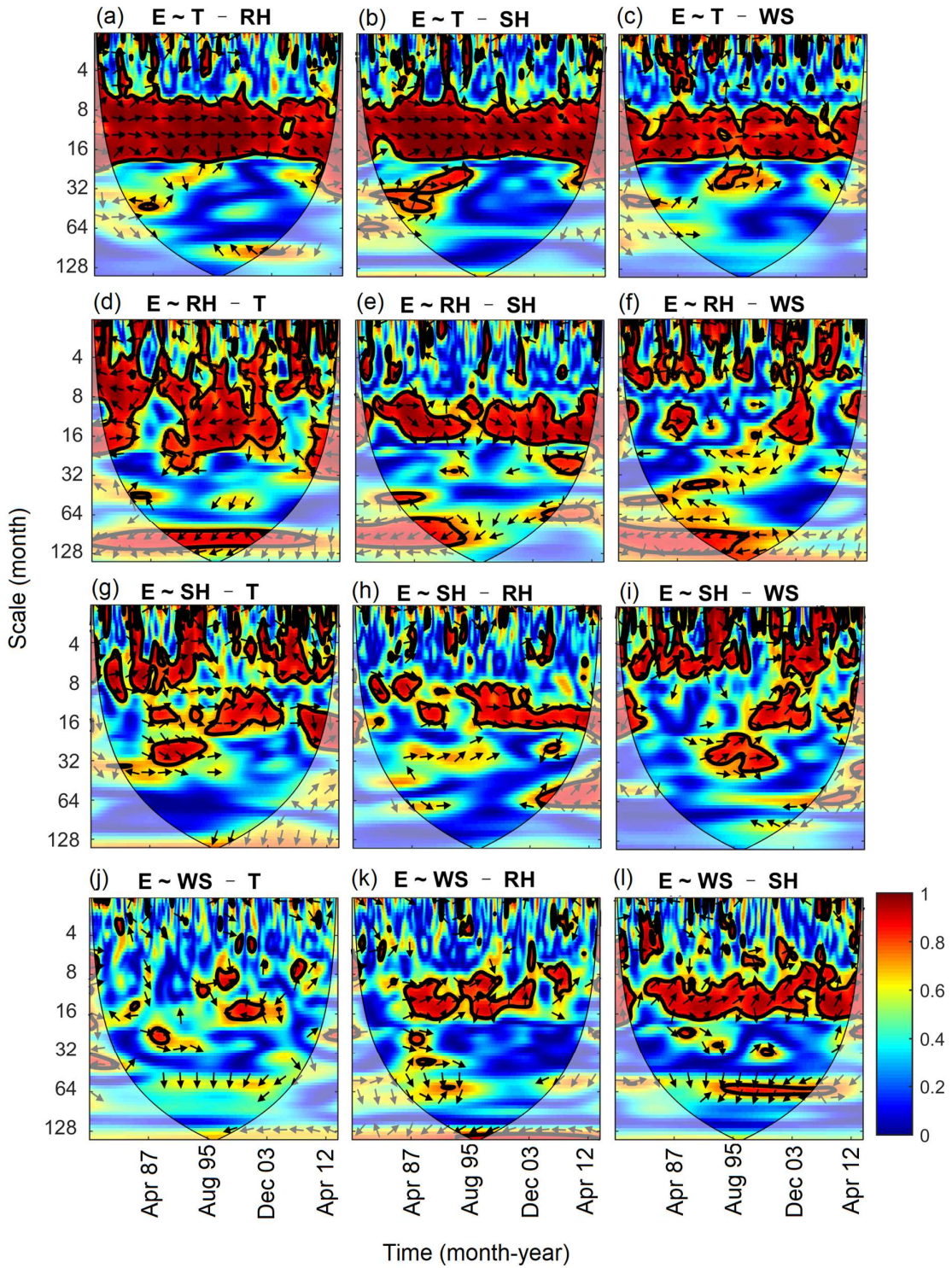
352 4.1 Description of free water evaporation dataset

353 The free water evaporation dataset was used to test MWC (Hu and Si, 2016). In brief,
 354 this dataset includes monthly free water evaporation (E), mean temperature (T), relative
 355 humidity (RH), sun hours (SH), and wind speed (WS) between January 1979 and December
 356 2013 at Changwu site in Shaanxi province provided by the China Meteorological
 357 Administration. During this period, the average daily temperature was 9.4 °C, the average

358 annual rainfall was 571 mm and annual potential evapotranspiration was 883 mm. Because
359 of its location between semi-arid and subhumid climates, agricultural production at the
360 Changwu site is constrained by water availability. Results of wavelet power spectrum of E
361 and BWC between every two variables are shown in Fig. S3 and Fig. S4 (Sect. S3 in the
362 Supplement), respectively.

363 **4.2 PWC with free water evaporation dataset**

364 The PWC analysis indicates that the correlations between E and T after excluding the
365 effect of each of other three variables (RH, SH, and WS) were almost the same as those
366 indicated by BWC (Fig. 3a-c and Fig. S4 of Sect. S3 in the Supplement). For example, E
367 and T, after excluding the effect of RH, were positively correlated at the medium scales (8–
368 32 months). The PASC was 61% and mean PWC_{sig} value was 0.94. No significant
369 correlations between E and T from 1979 to 1992 were found at scales around 64 months
370 after eliminating the influence of RH (Fig. 3a-c). This implies that the influence of mean
371 temperature on E at these scales and years may be associated with the negative influence of
372 RH on both E and T (Fig. S4 of Sect. S3 in the Supplement).



373

374 **Figure 3.**

375 Partial wavelet coherency (PWC) between evaporation (E) and each meteorological factor

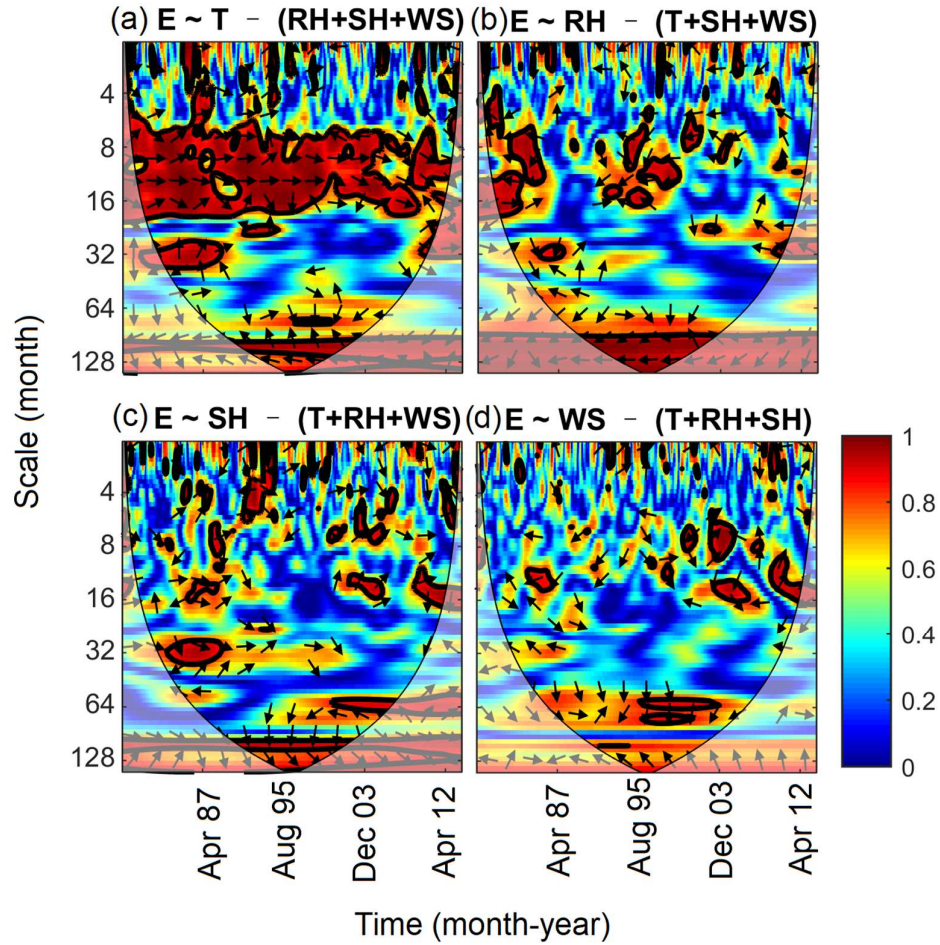
376 (T, mean temperature; RH, relative humidity; SH, sun hours; WS, wind speed) after
377 excluding the effect of each of other three meteorological factors.

378 PWC between E and RH depended on the excluding variable and scale (Fig. 3d-f). The
379 mean PWC and PASC between E and RH after excluding T were 0.60 and 34%, respectively,
380 which are comparable with the mean BWC (0.62) and PASC (40%) between E and RH.
381 The corresponding values after excluding SH and WS were 0.50 and 0.53 (PWC), 22% and
382 21% (PASC), respectively. In addition, compared with the BWC between E and RH (Fig.
383 S4 of Sect. S3 in the Supplement), correlations between E and RH were weak at small scales
384 (<8 months) and medium scales (8–32 months) after eliminating the influence of SH and
385 WS (Fig. 3e-f), respectively. Therefore, excluding the variable of T had less influence on
386 the coherence between E and RH compared with excluding the variables of SH and WS.
387 This is mainly because RH and T are correlated with E at different scales (Fig. S4 of Sect.
388 S3 in the Supplement), i.e., mean temperature affected E mainly at medium scales, while
389 RH affected E across all scales. However, the domain where SH and WS were correlated
390 with E was a subset of that where RH and E were correlated (Fig. S4 of Sect. S3 in the
391 Supplement).

392 The relationships between E and SH after excluding the other three factors were less
393 consistent (Fig. 3g-h). The areas with significant corrections were scattered over the whole
394 location-scale domain but differed with excluding factor. The PASC varied from 12%
395 (excluding RH) to 20% (excluding T and WS), which is much lower than the PASC (28%)
396 in the case of BWC. The significant relationships between E and WS were only limited to
397 very small areas except for the case of SH being excluded, where E and WS were positively

398 correlated at scales of 8–16 months most of the time (Fig. 3j-l).

399 In general, the PASC decreased after excluding the effects of more factors (data not
400 shown). The correlations between E and each variable after eliminating the effects of all
401 other variables are shown in Fig. 4. The correlations between E and T were still significant
402 at the medium scales (8–32 months) (Fig. 4a), where PASC value was 52% with mean
403 PWC_{sig} of 0.92. The E was still correlated with RH at large scales (>85 months) (Fig. 4b),
404 where PASC value was 35% with mean PWC_{sig} of 0.96. Interestingly, the domain with
405 significant correlation between E and SH and WS was very limited (Fig. 4c-d). This
406 indicates that the influences of SH and WS on E have already been covered by RH and T.
407 This is in agreement with the MWC results that RH and T were the best to explain E
408 variations at all scales (Hu and Si, 2016). Although the RH had the greatest mean wavelet
409 coherence and PASC at the entire location-scale domains, the PWC analysis seems to
410 support that mean temperature was the most dominating factor for free water evaporation
411 at the 1-year cycle (8–16 months), which is the dominant scale of E variation (Fig. S3 of
412 Sect. S3 in the Supplement).



413

414 **Figure 4.**

415 Partial wavelet coherency (PWC) between evaporation (E) and each meteorological factor
 416 (T, mean temperature; RH, relative humidity; SH, sun hours; WS, wind speed) after
 417 excluding the effects of all other three factors.

418 **5. Discussion on the advantages and weaknesses of the new method**

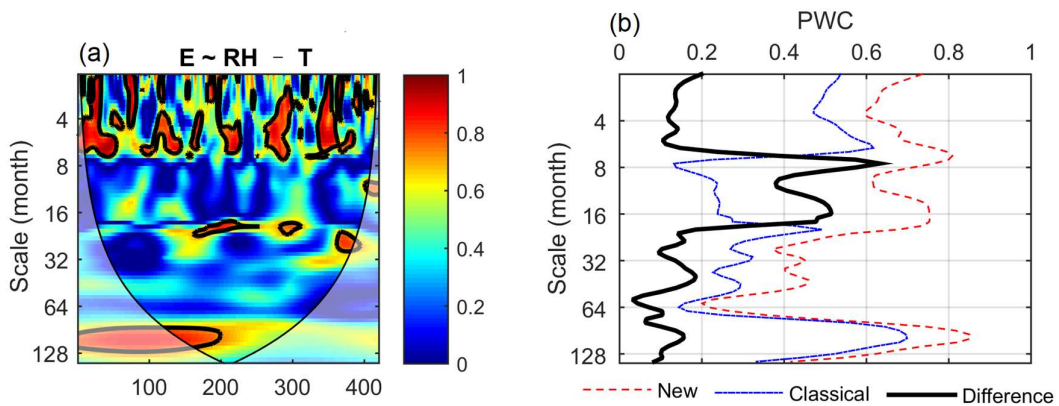
419 **5.1 Advantages**

420 We extend the partial coherence method from the frequency (scale) domain (Koopmans,
 421 1995) to the time-frequency (location-scale) domain. The new method is an extension of

422 previous work on PWC and MWC (Mihanović et al., 2009; Hu and Si, 2016). The method
423 test and application have verified that it has the advantage of dealing with more than one
424 excluding variable and providing the phase information associated with PWC. In the case
425 of one excluding variable, Mihanović et al. (2009) has suggested to calculate PWC by using
426 an equation analogous to the traditional partial correlation squared (Eq. 14), which can be
427 derived from our Eq. (9). However, their equation was, unfortunately, widely used by
428 replacing the complex coherence in Eq. (14) with real coherence as expressed in Eq. (15)
429 (Ng and Chan, 2012b, a; Rathinasamy et al., 2017; Aloui et al., 2018; Altarturi et al., 2018b;
430 Jia et al., 2018; Li et al., 2018; Mutascu and Sokic, 2020; Wu et al., 2020). This mistake is
431 corrected in this paper.

432 The differences between the new ~~calculation~~—(Eq.14) and the classical
433 ~~implementation~~ (Eq. 15) are compared in the case of one excluding variable
434 using both the artificial and real datasets. Except for the phase information, the two
435 ~~implementations~~ generally produce comparable coherence for the artificial
436 dataset (Fig. S5 of Sect. S3 in the Supplement). However, the new
437 ~~calculation~~ produces consistently and slightly higher coherence than the
438 classical ~~implementation~~. For example, their mean PWCs between y and y_2 at
439 the scale of 8 after excluding the effect of y_4 are 1.00 and 0.97, respectively. This indicates
440 that the new ~~calculation~~ produces coherence between y and y_2 at the scale
441 (8) of y_2 closer to 1 as we expect. While the classical ~~implementation~~ produces
442 similar PWC between E and other meteorological factors in most cases especially for the
443 coherence between E and T after excluding the effects of others (Fig. S6 of Sect. S3 in the

444 Supplement), large differences between these two implementations can also be
 445 observed. For example, while the new implementation recognizes the strong
 446 coherence between E and RH after excluding the effect of T at scales of around 1 year (Fig.
 447 3d), this coherence was negligible by the classical implementation (Fig. 5a).
 448 Mean PWC values by the new implementation were consistently higher than the
 449 classical implementation, and the differences ranged from 0.4 to 0.6 around the
 450 scale of 1 year (Fig. 5b). Considering the real coherence (Eq.15) rather than complex
 451 coherence (Eq.14) between every two variables in the numerators can potentially result in
 452 large underestimation of the partial wavelet coherence. Therefore, the ability of the new
 453 method and implementation to produce more accurate results than the classical
 454 implementation is one of its advantages.



455

456 **Figure 5.**

457 Partial wavelet coherency (PWC) between evaporation (E) and relative humidity (RH) after
 458 excluding the effect of mean temperature (T) using the classical implementation
 459 (Eq. 15) (a) and differences in PWC between the new implementation (Eq.14) and classical

460 implementation calculation as a function of scale (b).

461 Compared with the Mihanović et al. (2009) method, the additional phase information
462 from the new PWC is another advantage of this new method. This is because phase
463 information is directly related to the type of correlation, i.e., in-phase and out-of-phase
464 indicating positive and negative correlation, respectively. Different types of correlations
465 were usually found at different locations and scales (Hu et al., 2017b). The phase
466 information helps understand the differences in associated mechanisms or processes at
467 different locations and scales. In addition, the phase information will allow us to detect the
468 changes in not only the degree of correlation (i.e., coherence) but also the type of correlation
469 after excluding the effect of other variables. For example, E and RH were positively
470 correlated at the 1-year cycle (8–16 months) from year 1979 to 1995. This is because higher
471 evaporation usually occurs in summer when high T coincides with high RH as influenced
472 by the monsoon climate in the study area (Fig. S4 of Sect. S3 in the Supplement).
473 Interestingly, after excluding the effect of T, E was negatively correlated with RH at the
474 scale of 1 year as we expect (Fig. 3d).

475 Moreover, our new PWC method applies to cases with more than one excluding variable,
476 which is a knowledge gap. When multiple variables are correlated with both the predictor
477 and response variables, the correlations between predictor and response variables may be
478 misleading if the effects of all these multiple variables were not removed. For example, at
479 the dominant scale (i.e., 1 year) of E variation, contrasting effects of RH on E existed after
480 excluding the effects of T (negative) or SH (positive) (Fig. 3d-e). However, after the effects

481 of all other variables were excluded, there were negligible effects of RH on E at this scale
482 (Fig. 4b). In this case, the relationship between E and RH at the scale of 1 year can be
483 misleading after removing the effects of only one variable. In addition, the dominant role
484 of mean temperature in driving free water evaporation at the 1-year cycle was proved by
485 removing the effects of all other meteorological factors (Fig. 4a). This also further verifies
486 the suitability of the Hargreaves model (only air temperature and incident solar radiation
487 required) (Hargreaves, 1989) for estimating potential evapotranspiration on the Chinese
488 Loess Plateau (Li, 2012).

489 **5.2 Weaknesses**

490 The new method has the risk to produce spurious high correlations after excluding the
491 effect from other variables. Take the artificial dataset for example, at the scale of 32, PWC
492 values between y and y_2 after excluding y_4 are not significant, but relatively high, partly
493 because of small octaves per scale (octave refers to the scaled distance between two scales
494 with one scale being twice or half of the other, default of 1/12). This spurious unexpected
495 high PWC is caused by low values in both the numerator (partly associated with the low
496 coherence between response y and predictor variables y_2 at the scale of 32) and denominator
497 (partly associated with the high coherence between response y and excluding variable y_4 at
498 the scale of 32) in Eq. (9). The same problem also exists in the classical
499 ~~implementation calculation~~ implementation (Fig. S5 of Sect. S3 in the Supplement). So, caution should be
500 taken to interpret those results. However, it seems that the domain with spurious correlation
501 calculated by the new method is very limited and it is located mainly outside of the cones

502 of influence. Moreover, the unexpected results can be easily ruled out with knowledge of
503 BWC between response and predictor variables. It is expected that the correlation between
504 two variables should not increase after excluding one or more variables. Therefore, BWC
505 analysis is suggested for better interpretation of the PWC results.

506 Similar to BWC and MWC, the confidence level of PWC calculated from the Monte
507 Carlo simulation is based on a single hypothesis testing. But in reality, the confidence level
508 of PWC values at all locations and scales needs to be tested simultaneously. Therefore, the
509 significance test has the problem of multiple testing, i.e., more than one individual
510 hypothesis is tested simultaneously (Schaepli et al., 2007; Schulte et al., 2015). The new
511 method may benefit from a better statistical significance testing method. Options for
512 multiple testing can be the Bonferroni adjusted p test (Westfall and Young, 1993) or false
513 discovery rate (Abramovich and Benjamini, 1996; Shen et al., 2002), which is less stringent
514 than the former. The AR(1) model was used to generate noise series for testing the
515 confidence level of PWC. High-order autoregressive models rather than AR(1) may be
516 beneficial for a significance test where spatial data (or time series) ~~data~~ are characterized
517 by long-range dependence (Szolgayová et al., 2014).

518 **6. Conclusions**

519 Partial wavelet coherency (PWC) is ~~developed~~improved to investigate scale-specific and
520 localized bivariate relationships after excluding the effect of one or more variables in
521 geoscience. Method tests using stationary and non-stationary artificial datasets verified the
522 known scale- and localized bivariate relationships after eliminating the effects of other

523 variables. Compared with the previous PWC method, the new PWC method has the
524 advantage of dealing with more than one excluding variable and providing the phase
525 information (i.e., correlation type) associated with PWC. In the case of one excluding
526 variable, ~~this~~ the PWC implementation provided here (in the paper and the published code)
527 ~~new method~~ produces more accurate coherence than the previously published PWC
528 ~~calculation implementation~~ that considered wrongly only real coherence rather than
529 complex coherence between every two variables. Application of the new method to the real
530 dataset has further proved its robustness in untangling the bivariate relationships after
531 removing the effects of all other variables in multiple location-scale domains. The new
532 method provides a much needed data-driven tool for unraveling underlying mechanisms in
533 both temporal and spatial data. Thus, combining with wavelet transform, BWC, and MWC,
534 the new PWC method can be used to analyze various processes in geoscience, such as
535 stream flow, droughts, greenhouse gas emissions (e.g., N₂O, CO₂, and CH₄), atmospheric
536 circulation, and oceanic processes (e.g., El Niño-Southern Oscillation).

537 **Code/Data availability**

538 The Matlab codes for calculating PWC, along with the updated MWC codes, are freely
539 accessible (<https://figshare.com/s/bc97956f43fe5734c784>). The codes are developed based
540 on those provided by Aslak Grinsted (<http://www.glaciology.net/wavelet-coherence>). The
541 meteorological dataset can be obtained from the China Meteorological Administration.

542 **Author contributions**

543 WH wrote the paper, ~~did~~ developed the Matlab code ~~development~~, and analyzed the data.

544 Both authors conceived the study, interpreted the results, and revised the paper.

545 **Competing interests**

546 The authors declare that they have no conflict of interest.

547 **Acknowledgements**

548 The preparation of this manuscript was supported by The New Zealand Institute for Plant
549 and Food Research Limited under the Sustainable Agro-ecosystems programme.

550 **References**

551 Abramovich, F. and Benjamini, Y.: Adaptive thresholding of wavelet coefficients,
552 Computational Statistics & Data Analysis, 22, 351-361, 1996.

553 Aloui, C., Hkiri, B., Hammoudeh, S., and Shahbaz, M.: A multiple and partial wavelet
554 analysis of the oil price, inflation, exchange rate, and economic growth nexus in Saudi
555 Arabia, Emerging Markets Finance and Trade, 54, 935-956, 2018.

556 Altarturi, B. H., Alshammari, A. A., Saiti, B., and Erol, T.: A three-way analysis of the
557 relationship between the USD value and the prices of oil and gold: A wavelet analysis,
558 AIMS Energy, 6, 487, 2018a.

559 Altarturi, B. H. M., Alshammari, A. A., Saiti, B., and Erol, T.: A three-way analysis of the
560 relationship between the USD value and the prices of oil and gold: A wavelet analysis, Aims

561 Energy, 6, 487-504, 2018b.

562 Biswas, A. and Si, B. C.: Identifying scale specific controls of soil water storage in a
563 hummocky landscape using wavelet coherency, *Geoderma*, 165, 50-59, 2011.

564 Centeno, L. N., Hu, W., Timm, L. C., She, D. L., Ferreira, A. D., Barros, W. S., Beskow, S.,
565 and Caldeira, T. L.: Dominant Control of Macroporosity on Saturated Soil Hydraulic
566 Conductivity at Multiple Scales and Locations Revealed by Wavelet Analyses, *Journal of*
567 *Soil Science and Plant Nutrition*, 20, 2020.

568 Das, N. N. and Mohanty, B. P.: Temporal dynamics of PSR-based soil moisture across
569 spatial scales in an agricultural landscape during SMEX02: A wavelet approach, *Remote*
570 *Sensing of Environment*, 112, 522-534, 2008.

571 Graf, A., Bogena, H. R., Drüe, C., Hardelauf, H., Pütz, T., Heinemann, G., and Vereecken,
572 H.: Spatiotemporal relations between water budget components and soil water content in a
573 forested tributary catchment, *Water Resour Res*, 50, 4837-4857, 2014.

574 Grinsted, A., Moore, J. C., and Jevrejeva, S.: Application of the cross wavelet transform
575 and wavelet coherence to geophysical time series, *Nonlinear Processes in Geophysics*, 11,
576 561-566, 2004.

577 Gu, X. F., Sun, H. G., Tick, G. R., Lu, Y. H., Zhang, Y. K., Zhang, Y., and Schilling, K.:
578 Identification and Scaling Behavior Assessment of the Dominant Hydrological Factors of
579 Nitrate Concentrations in Streamflow, *J Hydrol Eng*, 25, 06020002, 2020.

580 Hargreaves, G. H.: Accuracy of estimated reference crop evapotranspiration, *Journal of*
581 *irrigation and drainage engineering*, 115, 1000-1007, 1989.

582 Hu, W., Chau, H. W., Qiu, W. W., and Si, B. C.: Environmental controls on the spatial

583 variability of soil water dynamics in a small watershed, *J Hydrol*, 551, 47-55, 2017a.

584 Hu, W. and Si, B. C.: Technical note: Multiple wavelet coherence for untangling scale-
585 specific and localized multivariate relationships in geosciences, *Hydrol Earth Syst Sc*, 20,
586 3183-3191, 2016.

587 Hu, W., Si, B. C., Biswas, A., and Chau, H. W.: Temporally stable patterns but seasonal
588 dependent controls of soil water content: Evidence from wavelet analyses, *Hydrol Process*,
589 31, 3697-3707, 2017b.

590 Jia, X., Zha, T., Gong, J., Zhang, Y., Wu, B., Qin, S., and Peltola, H.: Multi-scale dynamics
591 and environmental controls on net ecosystem CO₂ exchange over a temperate semiarid
592 shrubland, *Agricultural and Forest Meteorology*, 259, 250-259, 2018.

593 Kenney, J. F. and Keeping, E. S.: *Mathematics of Statistics*, D. van Nostrand, 1939.

594 Koopmans, L. H.: *The spectral analysis of time series*, Elsevier, 1995.

595 Lakshmi, V., Piechota, T., Narayan, U., and Tang, C.: Soil moisture as an indicator of
596 weather extremes, *Geophysical research letters*, 31, L11401, 2004.

597 Li, H., Dai, S., Ouyang, Z., Xie, X., Guo, H., Gu, C., Xiao, X., Ge, Z., Peng, C., and Zhao,
598 B.: Multi-scale temporal variation of methane flux and its controls in a subtropical tidal salt
599 marsh in eastern China, *Biogeochemistry*, 137, 163-179, 2018.

600 Li, Z.: Applicability of simple estimating method for reference crop evapotranspiration in
601 Loess Plateau, *Transactions of the Chinese Society of Agricultural Engineering*, 28, 106-
602 111, 2012.

603 Mares, I., Mares, C., Dobrica, V., and Demetrescu, C.: Comparative study of statistical
604 methods to identify a predictor for discharge at Orsova in the Lower Danube Basin,

605 Hydrological Sciences Journal, 65, 371-386, 2020.

606 Mihanović, H., Orlić, M., and Pasarić, Z.: Diurnal thermocline oscillations driven by tidal
607 flow around an island in the Middle Adriatic, Journal of Marine Systems, 78, S157-S168,
608 2009.

609 Mutascu, M. and Sokic, A.: Trade openness-CO₂ emissions nexus: a wavelet evidence from
610 EU, Environmental Modeling & Assessment, 25, 1-18, 2020.

611 Nalley, D., Adamowski, J., Biswas, A., Gharabaghi, B., and Hu, W.: A multiscale and
612 multivariate analysis of precipitation and streamflow variability in relation to ENSO, NAO
613 and PDO, J Hydrol, 574, 288-307, 2019.

614 Ng, E. K. and Chan, J. C.: Geophysical applications of partial wavelet coherence and
615 multiple wavelet coherence, Journal of Atmospheric and Oceanic Technology, 29, 1845-
616 1853, 2012a.

617 Ng, E. K. and Chan, J. C.: Interannual variations of tropical cyclone activity over the north
618 Indian Ocean, International Journal of Climatology, 32, 819-830, 2012b.

619 Polansky, L., Wittemyer, G., Cross, P. C., Tambling, C. J., and Getz, W. M.: From moonlight
620 to movement and synchronized randomness: Fourier and wavelet analyses of animal
621 location time series data, Ecology, 91, 1506-1518, 2010.

622 Rathinasamy, M., Agarwal, A., Parmar, V., Khosa, R., and Bairwa, A.: Partial wavelet
623 coherence analysis for understanding the standalone relationship between Indian
624 Precipitation and Teleconnection patterns, arXiv preprint arXiv:1702.06568, 2017. 2017.

625 Schaepli, B., Maraun, D., and Holschneider, M.: What drives high flow events in the Swiss
626 Alps? Recent developments in wavelet spectral analysis and their application to hydrology,

627 Adv Water Resour, 30, 2511-2525, 2007.

628 Schulte, J., Duffy, C., and Najjar, R.: Geometric and topological approaches to significance
629 testing in wavelet analysis, *Nonlinear Processes in Geophysics*, 22, 2015.

630 Sen, A., Chaudhury, P., and Dutta, K.: On the co-movement of crude, gold prices and stock
631 index in Indian market, arXiv preprint arXiv:1904.05317, 2019. 2019.

632 Shen, X., Huang, H.-C., and Cressie, N.: Nonparametric hypothesis testing for a spatial
633 signal, *Journal of the American Statistical Association*, 97, 1122-1140, 2002.

634 Si, B. C.: Spatial scaling analyses of soil physical properties: A review of spectral and
635 wavelet methods, *Vadose Zone Journal*, 7, 547-562, 2008.

636 Si, B. C. and Farrell, R. E.: Scale-dependent relationship between wheat yield and
637 topographic indices: A wavelet approach, *Soil Sci Soc Am J*, 68, 577-587, 2004.

638 Si, B. C. and Zeleke, T. B.: Wavelet coherency analysis to relate saturated hydraulic
639 properties to soil physical properties, *Water Resour Res*, 41, W11424, 2005.

640 Song, X. M., Zhang, C. H., Zhang, J. Y., Zou, X. J., Mo, Y. C., and Tian, Y. M.: Potential
641 linkages of precipitation extremes in Beijing-Tianjin-Hebei region, China, with large-scale
642 climate patterns using wavelet-based approaches, *Theoretical and Applied Climatology*,
643 141, 1251-1269, 2020.

644 Su, L., Miao, C., Duan, Q., Lei, X., and Li, H.: Multiple - wavelet coherence of world's
645 large rivers with meteorological factors and ocean signals, *Journal of Geophysical Research:*
646 *Atmospheres*, 124, 4932-4954, 2019.

647 Szolgayová, E., Arlt, J., Blöschl, G., and Szolgay, J.: Wavelet based deseasonalization for
648 modelling and forecasting of daily discharge series considering long range dependence, *J*

649 Hydrol Hydromech, 62, 24-32, 2014.

650 Tan, X., Gan, T. Y., and Shao, D.: Wavelet analysis of precipitation extremes over Canadian
651 ecoregions and teleconnections to large - scale climate anomalies, Journal of Geophysical
652 Research: Atmospheres, 121, 14469-14486, 2016.

653 Torrence, C. and Compo, G. P.: A practical guide to wavelet analysis, Bulletin of the
654 American Meteorological society, 79, 61-78, 1998.

655 Wendroth, O., Alomran, A. M., Kirda, C., Reichardt, K., and Nielsen, D. R.: State-Space
656 Approach to Spatial Variability of Crop Yield, Soil Sci Soc Am J, 56, 801-807, 1992.

657 Westfall, P. H. and Young, S. S.: Resampling-based multiple testing: Examples and methods
658 for p-value adjustment, John Wiley & Sons, 1993.

659 Wu, K., Zhu, J., Xu, M., and Yang, L.: Can crude oil drive the co-movement in the
660 international stock market? Evidence from partial wavelet coherence analysis, The North
661 American Journal of Economics and Finance, 2020. 101194, 2020.

662 Yan, R. and Gao, R. X.: A tour of the tour of the Hilbert-Huang transform: an empirical tool
663 for signal analysis, IEEE Instrumentation & Measurement Magazine, 10, 40-45, 2007.

664 Zhao, R., Biswas, A., Zhou, Y., Zhou, Y., Shi, Z., and Li, H.: Identifying localized and scale-
665 specific multivariate controls of soil organic matter variations using multiple wavelet
666 coherence, Sci Total Environ, 643, 548-558, 2018.

667